

Abnormal Gene Expression Profiles in Human Ovaries from Polycystic Ovary Syndrome Patients

ERIK JANSEN, JOOP S. E. LAVEN, HENRI B. R. DOMMERHOLT, JAN POLMAN, CINDY VAN RIJT, CAROLINE VAN DEN HURK, JOLANDA WESTLAND, SIETSE MOSSELMAN, AND BART C. J. M. FAUSER

Global Business Intelligence Center (E.J.); Department of Molecular Design and Informatics (J.P.); and Target Discovery Unit (C.v.R., C.v.d.H., J.W.), Department of Pharmacology (S.M.), NV Organon, 5340 BH Oss; Center of Reproductive Medicine (J.S.E.L., B.C.J.M.F.), Erasmus Medical Center, 3000 CA Rotterdam; Department of Obstetrics and Gynecology (H.B.R.D.), Flevohospital, 1315 RA Almere; and Department of Reproductive Medicine (B.C.J.M.F.), University Medical Center Utrecht, 3508 GA Utrecht, The Netherlands

Polycystic ovary syndrome (PCOS) represents the most common cause of anovulatory infertility and affects 5–10% of women of reproductive age. The etiology of PCOS is still unknown. The current study is the first to describe consistent differences in gene expression profiles in human ovaries comparing PCOS patients vs. healthy normoovulatory individuals. The microarray analysis of PCOS vs. normal ovaries identifies dysregulated expression of genes encoding components of several biological pathways or systems such as Wnt signaling, extracellular matrix components, and immunolog-

ical factors. Resulting data may provide novel clues for ovarian dysfunction in PCOS. Intriguingly, the gene expression profiles of ovaries from (long-term) androgen-treated female-to-male transsexuals (TSX) show considerable overlap with PCOS. This observation provides supportive evidence that androgens play a key role in the pathogenesis of PCOS. Presented data may contribute to a better understanding of dysregulated pathways in PCOS, which might ultimately reveal novel leads for therapeutic intervention. (*Molecular Endocrinology* 18: 3050–3063, 2004)

THE CURRENTLY ACCEPTED clinical definition of the polycystic ovary syndrome (PCOS) involves the combination of chronic anovulation, clinical and endocrinological signs of hyperandrogenism, and polycystic ovaries (PCO) assessed by ultrasound (1, 2). Serum LH levels are frequently elevated in these patients, and it has become evident that hyperinsulinemia can be observed in at least 50% of the PCOS population. PCOS represents the most common cause of anovulatory infertility (3), and the prevalence of this condition in women of reproductive age has been estimated to be around 5–10% (4, 5).

In PCOS ovaries, growth of early antral follicles is typically arrested at the 5- to 10-mm stage, resulting in

ovaries with multiple follicular structures less than 10 mm in diameter (6, 7). The volume and density of the ovarian stroma are increased (8), and there is rarely evidence of recent ovulations. The number of primordial follicles is similar compared with normal ovaries. An increased amount of ripening as well as atretic 2- to 10-mm follicles can be observed (9, 10), which is supported by recent observations indicating elevated serum concentrations of anti-Müllerian hormone, a specific marker for preantral and early antral ovarian follicles, in these patients (11). Studies involving PCOS theca cells in culture have documented a biochemical (12) and molecular (13) phenotype distinctly different from cells derived from regularly cycling women.

The existing literature indicates familial clustering of PCOS (14). The mode of inheritance of the disorder is still uncertain. Although initially a single autosomal-dominant pattern of transmission was proposed, recent studies are indicative of a more complex mode of inheritance (15,16). Genetic studies have been hampered due to heterogeneity in the phenotype of PCOS patients. Moreover, the availability of only small numbers of sibpairs and the lack of an unambiguous male phenotype along with the absence of an appropriate animal model have complicated the elucidation of the genetic basis of PCOS. Most genetic studies undertaken so far have taken a candidate gene approach in cultures of isolated cells, focusing on genes involved in folliculogenesis [myeloid cell leukemia-1 (17),

Abbreviations: AD, Androstenedione; ADAMTS-1, a disintegrin and metalloprotease with thrombospondin motifs-1; BMI, body mass index; C/EBP β , CCAAT enhancer binding protein β ; DHEA, dehydroepiandrosterone; DHEAS, dehydroepiandrosteronesulfate; DUSP1, dual specificity phosphatase 1; E₂, estradiol; ECM, extracellular matrix; FAI, free androgen index; HDAC, histone deacetylase; MHC, major histocompatibility complex; NGF, nuclear growth factor; PCA, principal component analysis; PCO, polycystic ovaries; PCOS, polycystic ovary syndrome; PPAR, peroxisome proliferator-activated receptor; SGK, serum and glucocorticoid-regulated kinase; SHBG, sex hormone-binding globulin; T, testosterone; TSX, androgen-treated female-to-male transsexual; VPA, valproic acid.

***Molecular Endocrinology* is published monthly by The Endocrine Society (<http://www.endo-society.org>), the foremost professional society serving the endocrine community.**

growth differentiation factor-9 (18), or plasma protein A (19)], steroidogenesis [such as steroid acute regulatory protein (20), or cytochrome P450 17 (21, 22)] and genes involved in insulin signaling (23–25). As stated earlier, it seems highly likely that a multigenic defect is to be held responsible for PCOS. However, to date, there are no studies that describe genes specifically linked to PCOS susceptibility.

Today's technology (e.g. microarray analysis) enables us to generate a gene expression profile in any given tissue or cell type of interest (26, 27). It is therefore possible to assess the expression pattern of tens of thousands of genes in a single experiment. This experimental approach represents a new method to define the molecular phenotype of a disease. Moreover, this technology has recently been used successfully to identify altered gene expression in other disease conditions such as multiple sclerosis (28) and type 2 diabetes (29). The current study describes the first analysis of differences in gene expression profiles in ovarian tissue obtained from PCOS patients, female-to-male transsexuals, and normoovulatory individuals. Abnormal pathways are identified in PCOS, which may potentially lead to the identification of candidate genes for subsequent evaluation. Consequently, these transcription profiles might reveal novel critical information regarding the molecular basis of ovarian dysfunction in PCOS patients.

Because there is no suitable animal model, we took advantage of several interesting observations in humans that were reported more than a decade ago. It has been described that the ovarian morphology (30) and endocrine profile (7) in long-term androgen-treated female-to-male transsexuals (TSX) resembles PCOS, providing supportive evidence that androgens play a critical role in the pathogenesis of PCOS. However, these similarities between PCOS and TSX ovaries were described at the level of morphology and endocrinology. No studies address changes in both PCOS and TSX at the molecular level. The TSX may represent a unique human model for the study of PCOS despite the fact that TSX ovaries are smaller with more atretic follicles (presumably due to suppressed gonadotropins resulting from exogenous androgen administration).

The comparison of gene expression profiles between PCOS and normal ovaries may also reveal novel information regarding genes associated with early and later stages of antral follicle development, ovulation, and corpus luteum formation under normal conditions. Moreover, the identification of pathways that are abnormal in PCOS may contribute to the understanding of the pathogenesis of PCOS and might reveal novel avenues for therapeutic intervention.

RESULTS

Subjects

The control group consisted of 11 women with a median age of 38 yr (range, 35.5–40.0). Control group

women had a median body mass index (BMI) of 24.3 (range, 21.9–33.6 kg/m²) and a median cycle duration of 28 (range, 28–34 d). Endocrine and ultrasound data were not available because these characteristics were not recorded in these women. Ten of 11 women had a BRCA1 mutation, and only one woman had a familial history of breast cancer without having a BRCA1 or -2 mutation. Ovaries were collected either during the follicular phase (n = 7) or during the luteal phase (n = 4) of the menstrual cycle. Histological evaluation revealed that, although scant, developing follicles were still present in all ovaries, and the ovarian stromal compartment appeared normal (data not shown). From normoovulatory controls, one ovary was analyzed randomly by microarray. In total, 11 randomly chosen normal ovary samples were analyzed in the present study.

The PCOS patient group consisted of six women with a median age of: 29.8 yr (range, 27.3–32.4). Their median BMI was 20.9 kg/m², ranging from 17.7 to 33.5 kg/m². PCOS women had a median bleeding interval of 160 d ranging from 90–199 d. Three of six women (50%) were amenorrheic, whereas the other three were oligomenorrheic. LH serum levels were elevated (median, 12.8 IU/liter; range, 5.8–18.1), whereas FSH concentrations were within the normal range (median, 5.5 IU/liter; range, 4.5–7.5). Median T levels were 2.6 nmol/liter (range, 1.1–3.2) being within the normal range. The free androgen index (FAI) was elevated (i.e. 5.5; range, 1.1–13.5). The mean ovarian volume in PCOS patients was increased (i.e. 20.6 ml; range, 11.7–53.0) as was the total follicle number (median, 42; range, 22–60). Ovarian biopsies were collected randomly because these patients did not have a regular menstrual cycle. Histological evaluation of two samples revealed the characteristic histological PCOS picture showing multiple small subcortical follicles and an increased stromal hyperplasia (data not shown). In two of six PCOS women, both biopsies were analyzed whereas in the remaining four patients only one biopsy, randomly chosen, was processed for microarray analysis.

The TSX group consisted of 15 female-to-male transsexuals (TSX) aged between 20 and 43 yr with a median age of 29.5 yr. Their median BMI was 24.2 kg/m² ranging from 20–33 kg/m². TSX subjects had a median menstrual cycle length of 28 d ranging from 26–32 d. Median LH and FSH serum concentrations, before testosterone (T) treatment was initiated, were 4.2 IU/liter (range, 1.1–7.1) and 2.5 IU/liter (range, 2.5–7.0), respectively. T levels before T therapy were within the normal range (i.e. 1.8 nmol/liter; range, 1.0–2.6). Ovaries were collected at random because these patients did lack regular menstrual periods due to the exogenous androgen therapy. Histological evaluation revealed multiple cystic follicles and pronounced theca cell hyperplasia in all ovaries (data not shown). In seven of 15 TSX subjects both ovaries were analyzed, whereas in the remaining eight patients only one

ovary, randomly chosen, was processed for microarray analysis.

There was a significant difference in age ($P < 0.001$) between normoovulatory controls, on one hand, and PCOS women and TSX individuals, on the other. There was no significant difference in BMI between the three groups. Comparing endocrine data from PCOS patients with those in TSX subjects revealed a significant difference ($P < 0.001$) in LH levels, whereas FSH, T and 17β -estradiol (E_2) levels were similar. The FAI was significantly ($P < 0.001$) higher in PCOS women compared with TSX subjects.

Microarray Data Analysis

We compared the gene expression profiles of the luteal- and follicular-phase samples of the normal women. The principal component analysis indicated that there are no major differences between the two samples. The sets do not form two different groups, *i.e.* they do not constitute two separate entities within the control sample group (data not shown).

In addition, to substantiate the relative normality of our control samples, we compared our gene array data with the gene array data as present in the so-called GeneExpress datasuite from GeneLogic, Gaithersburg, MD (www.genelogic.com). The resulting gene expression profiles matched very well with the data obtained within our controls (*i.e.* comparable list of regulated genes).

To assess whether we would be able to identify expression profiles indicative of a molecular signature of PCOS ovaries, we performed a principal component analysis (PCA). The PCA was performed for all ovary samples using the normalized fluorescence intensity data from 500 representative transcripts. PCA reduces redundant variables in complex data sets to principal components that represent the majority of the variability in the data (31). When the PCA data are plotted, the eight PCOS samples cluster together within a discrete region that is clearly distinct from the 11 normal ovary samples (Fig. 1). In addition, the 22 TSX samples are clustered close to the PCOS samples. A distinctly different gene expression profile of one particular PCOS individual can be observed in Fig. 1. Interestingly, this patient is the only patient that conceived spontaneously after bilateral ovarian biopsies were taken. She also experienced a severe ovarian hyperstimulation syndrome twice during previous ovulation induction using gonadotropins in a low-dose step-up protocol.

Subsequently, a scatter plot analysis was performed (Fig. 2). The two diagonals indicate the 1.8-fold cutoff in differential expression. Briefly, the data show that 78% of the regulated genes are expressed at a lower level in PCOS (Fig. 2A), compared with the normal samples. In addition, in TSX ovaries 66% of the regulated genes are also expressed at a lower level compared with normal samples (Fig. 2B). Moreover, TSX

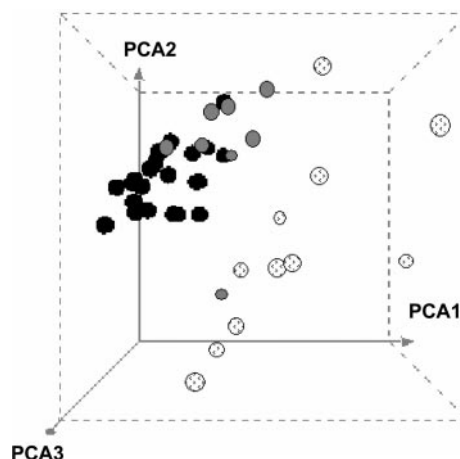


Fig. 1. PCA of PCOS, TSX, and Normal Ovaries

A representative set of 500 Affymetrix probe fragments was selected by K-means clustering. The resulting table was transposed and PCA was performed to detect and reduce the number variables to three principal components, which represent the majority of the variability in the dataset. A three-dimensional scatterplot was produced to visualize the differences in gene expression profiles comparing ovarian tissue obtained from regularly cycling women (*open circles*), PCOS (*gray circles*), and TSX (*black circles*).

samples do show a similar expression pattern as PCOS samples.

Analysis of Regulated Genes

The hybridization signal intensity of 230-probe fragments fulfills the selection criteria of: 1) the PCOS-to-normal ratio as being more than 1.8 or less than 0.55, and 2) the corresponding P value for the PCOS-to-normal being ≤ 0.01 . These fold-change levels of differential expression are average ratios resulting from consistent changes in many samples. Due to redundancy of the oligonucleotide probes on the U133A and U133B chips, the 230-probe fragments represented 189 genes that are differentially expressed in PCOS as compared with the controls. Several structure-function categories were represented in the list of differentially expressed genes including, for example, membrane receptors, transcription factors, and extracellular matrix (ECM) components. Several genes could be classified into specific signal transduction cascades or gene networks. Some of these genes and their role in ovarian function, such as nuclear growth factor I-B (NGFI-B) (32), CCAAT enhancer binding protein β (C/EBP β) (33), p21Cip (34), and serum and glucocorticoid-regulated kinase (SGK) (35), have been described previously. In Table 1 we have listed all the genes that are differentially expressed in PCOS ovaries, and we have also included the corresponding expression profile of TSX ovaries. The data show that the majority of PCOS-deregulated genes are also deregulated in TSX, confirming the PCA data. When analyzing the regulated genes for their chromosomal location, it becomes apparent that

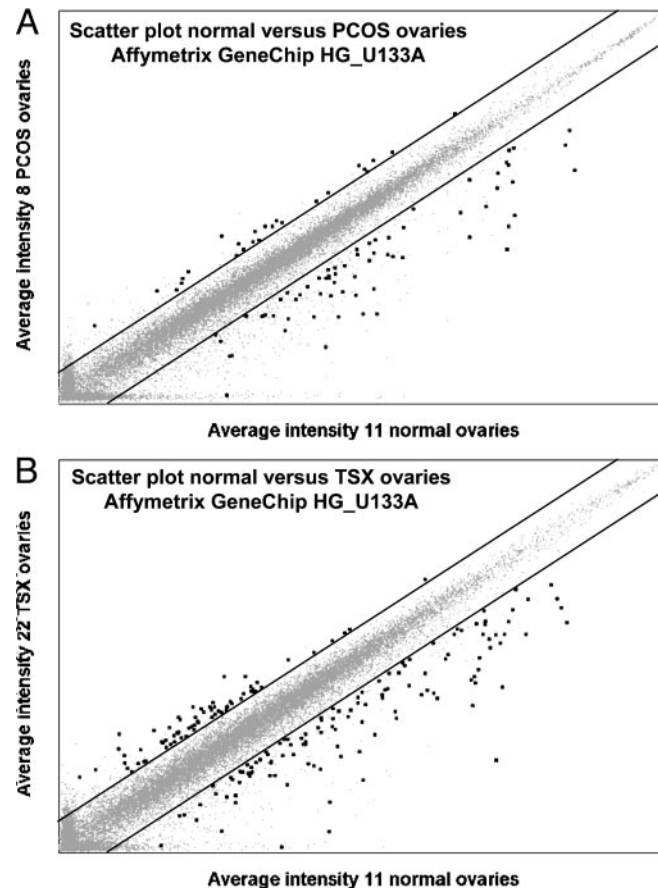


Fig. 2. Scatter Plot of Gene Expression in PCOS Ovaries and TSX Ovaries Compared with Regularly Cycling Controls

Probe fragments that are differentially expressed in PCOS ovaries (A) and in TSX ovaries (B) are depicted as **bold dots**. The selection criteria as described in *Materials and Methods* were applied. *Gray dots* indicate the probe fragments that do not comply with these selection criteria. The two *diagonals* indicate the 1.8-fold cutoff in differential expression.

multiple chromosomes are more frequently involved. When corrected for chromosome size and each chromosome's individual total predicted gene content, the PCOS-regulated genes are most frequently found on chromosome 6, 8, 14, 19, 21, 22, and, to a somewhat lesser extent, on chromosome 14 (Fig. 3). Moreover, chromosome 19 displays the highest relative score.

As can be deduced from Table 1, it is striking to see that many genes, such as Jun D, Fra-2, and EGR-1, which have a lower expression in PCOS and TSX ovaries, are positive regulators of cell proliferation. As to be expected, several genes, such as SGK and p21Cip, which are activated by the LH surge or which are predominantly expressed in preovulatory follicles, are decreased in PCOS ovaries.

Microarray Data Validation

Using real-time quantitative PCR, we have validated five gene transcript expression levels that were altered at least 1.8-fold in microarray analysis (Fig. 4). For each of the five genes, mRNA levels in qualitative PCR (Q-PCR) showed trends similar to those of the microarray experiment in both PCOS and TSX

samples. In addition, because it has been shown that sFrp4 is up-regulated in luteinized granulosa cells (36) and sFrp4 was not found in our list of regulated genes (Table 1), we performed a Q-PCR experiment to verify this. The results indicate no differential expression in normal ovaries compared with PCOS and TSX (data not shown). Therefore, the deselection of sFrp4 is not the result of too-stringent selection and cutoff criteria that we applied in generating the list of regulated genes but seems to represent a real phenomenon.

DISCUSSION

This is the first study to describe the transcriptome of ovaries from regularly cycling women, to identify changes at the molecular level comparing PCOS and normal ovaries, and to compare these abnormal gene expression profiles with those induced in TSX ovaries as a result of exogenous androgen exposure. We demonstrate that modest but distinct and consistent differences exist in gene expression profiles compar-

Table 1. Differences in Gene Transcript Levels in PCOS Ovaries and TSX Ovaries Compared with Regularly Cycling Controls

| Sequence Code | Title | Primary Sequence Name | FC N vs PCOS | FC N vs TSX | Location | Suppl. Info |
|---|---|-----------------------|--------------|--------------|---------------|-------------|
| Protein modifiers | | | | | | |
| 201044_x_at | dual specificity phosphatase 1 | DUSP1 | -28.73 | -9.48 | 5q34 | MK/LH |
| 201041_s_at | dual specificity phosphatase 1 | DUSP1 | -3.48 | -3.49 | 5q34 | MK/LH |
| 202014_at | protein phosphatase 1, regulatory (inhibitor) subunit 15A | PPP1R15A | -4.66 | -4.78 | 19q13.2 | AP |
| 37028_at | protein phosphatase 1, regulatory (inhibitor) subunit 15A | PPP1R15A | -3.41 | -4.03 | 19q13.2 | AP |
| 213975_s_at | lysozyme (renal amyloidosis) | FLJ23356 | -8.33 | -2.41 | 12q14.3 | |
| 224917_at | cathepsin D (lysosomal aspartyl protease) | VMP1 | -2.16 | -2.12 | 17q23.2 | |
| 211062_s_at | carboxypeptidase Z | CPZ | 2.08 | 1.6 | 4p16.1 | WN |
| 224567_x_at | histone deacetylase 3 | HDAC3 | -2.35 | 1.46 | 14q32.33 | |
| 200884_at | creatine kinase, brain | CKB | -3.17 | -2.03 | 14q32 | |
| 238987_at | UDP-Gal:betaGlcNAc beta 1,4- galactosyltransferase, polypeptide | B4GALT1 | -2.38 | -1.72 | 9p21.1 | |
| 204044_at | quinolinate phosphoribosyltransferase (nicotinate-nucleotide pyro | QPR1 | -2.21 | -1.61 | 16p12.1 | |
| 227627_at | serum/glucocorticoid regulated kinase-like | SGKL | -1.85 | -1.18 | 8q12.3-8q13.1 | |
| 203921_at | carbohydrate (N-acetylglucosamine-6-O) sulfotransferase 2 | CHST2 | 2.03 | 1.12 | 3q24 | |
| Heat shock proteins | | | | | | |
| 200664_s_at | DnaJ (Hsp40) homolog, subfamily B, member 1 | DNAJB1 | -8.89 | -6.1 | 19p13.2 | SR |
| 200666_s_at | DnaJ (Hsp40) homolog, subfamily B, member 1 | DNAJB1 | -3.76 | -3.84 | 19p13.2 | SR |
| 117_at | heat shock 70kDa protein 6 (HSP70B) | HSPA6 | -5.63 | -4.73 | 1cen-qter | SR |
| 200800_s_at | heat shock 70kDa protein 1A | HSPA1A | -4.96 | -4.6 | 6p21.3 | SR |
| 200799_at | heat shock 70kDa protein 1A | HSPA1A | -2.52 | -2.5 | 6p21.3 | SR |
| 202581_at | heat shock 70kDa protein 1B | HSPA1B | -3.82 | -3.58 | 6p21.3 | SR |
| 211969_at | heat shock 90kDa protein 1, alpha | HSPCA | -1.99 | -1.3 | 14q32.33 | SR |
| Transcription factors / DNA binding proteins | | | | | | |
| 204621_s_at | nuclear receptor subfamily 4, group A, member 2 | NR4A2 | -14.07 | -5.41 | 2q22-q23 | LH |
| 216248_s_at | nuclear receptor subfamily 4, group A, member 2 | NR4A2 | -7.37 | -5.14 | 2q22-q23 | LH |
| 204622_x_at | nuclear receptor subfamily 4, group A, member 2 | NR4A2 | -5.77 | -4.54 | 2q22-q23 | LH |
| 211143_x_at | nuclear receptor subfamily 4, group A, member 1 | NR4A1 (NGFI-B) | -9.99 | -9.4 | 12q13 | PR/LH |
| 202340_x_at | nuclear receptor subfamily 4, group A, member 1 | NR4A1 (NGFI-B) | -6.87 | -9.03 | 12q13 | PR/LH |
| 202672_s_at | activating transcription factor 3 | ATF3 | -9.62 | -4.8 | 1q32.3 | LH |
| 202768_at | FBJ murine osteosarcoma viral oncogene homolog B | FOSB | -7.86 | -31.12 | 19q13.32 | PR |
| 209189_at | v-fos FBJ murine osteosarcoma viral oncogene homolog | FOS | -6.07 | -6.02 | 14q24.3 | PR |
| 201465_s_at | v-jun sarcoma virus 17 oncogene homolog (avian) | JUN | -7.29 | -16.09 | 1p32-p31 | PR |
| 201464_x_at | v-jun sarcoma virus 17 oncogene homolog (avian) | JUN | -3.77 | -5.33 | 1p32-p31 | PR |
| 213281_at | v-jun sarcoma virus 17 oncogene homolog (avian) | JUN | -1.97 | -2.16 | 1p32-p31 | PR |
| 201473_at | jun B proto-oncogene | JUNB | -3.65 | -4 | 19p13.2 | PR/LH |
| 214326_x_at | jun D proto-oncogene | JUND | -2.54 | -3.82 | 19p13.2 | LH |
| 203751_x_at | jun D proto-oncogene | JUND | -2.09 | -4.13 | 19p13.2 | LH |
| 209304_x_at | growth arrest and DNA-damage-inducible, beta | GADD45B | -4.61 | -3.72 | 19p13.3 | AP/LH |
| 207574_s_at | growth arrest and DNA-damage-inducible, beta | GADD45B | -4.09 | -3.29 | 19p13.3 | AP/LH |
| 209305_s_at | growth arrest and DNA-damage-inducible, beta | GADD45B | -2.98 | -2.48 | 19p13.3 | AP/LH |
| 201693_s_at | early growth response 1 | EGR1 | -4.2 | -8.87 | 5q31.1 | LH |
| 201694_s_at | early growth response 1 | EGR1 | -2.76 | -4.3 | 5q31.1 | LH |
| 201236_s_at | BTG family, member 2 | BTG2 | -4.01 | -4.99 | 1q32 | PR |
| 201235_s_at | BTG family, member 2 | BTG2 | -2.47 | -2.65 | 1q32 | PR |
| 226646_at | Kruppel-like factor 2 (lung) | KLF2 | -3.15 | -2.71 | 19p13.13-p13 | LH |
| 219371_s_at | Kruppel-like factor 2 (lung) | KLF2 | -2.08 | -2.01 | 19p13.13-p13 | LH |
| 220266_s_at | Kruppel-like factor 4 (gut) | KLF4 | -3.68 | -4.26 | 9q31.2 | PR/LH |
| 221841_s_at | Kruppel-like factor 4 (gut) | KLF4 | -3.08 | -2.81 | 9q31.2 | PR/LH |
| 212501_at | CCAAT/enhancer binding protein (C/EBP), beta | CEBPB | -1.97 | -2.14 | 20q13.1 | LH |
| 213006_at | CCAAT/enhancer binding protein (C/EBP), delta | CEBPD | -2.07 | -2.35 | 8p11.2-p11.1 | |
| 203973_s_at | CCAAT/enhancer binding protein (C/EBP), delta | CEBPD | -1.8 | -2.03 | 8p11.2-p11.1 | |
| 203574_at | nuclear factor, interleukin 3 regulated | NFIL3 | -1.9 | -1.62 | 9q22 | |
| 201170_s_at | basic helix-loop-helix domain containing, class B, 2 | BHLHB2 | -2.66 | -2.41 | 3p26 | |
| 202081_at | immediate early protein | ETR101 | -2.39 | -3.25 | 19p13.12 | PR |
| 209967_s_at | cAMP responsive element modulator | CREM | -2.29 | -1.55 | 10p12.1-p11.1 | |
| 219228_at | zinc finger protein 463 | ZNF463 | -2.22 | -1.36 | 19q13.3-q13.4 | |
| 205372_at | pleomorphic adenoma gene 1 | PLAG1 | -1.84 | -1.3 | 8q12 | |
| 204069_at | Meis1, myeloid ecotropic viral integration site 1 homolog (mouse) | MEIS1 | -1.94 | -1.33 | 2p14-p13 | |
| 204931_at | transcription factor 21 | TCF21 | 1.88 | 1.14 | 6pter-qter | |
| 208510_s_at | peroxisome proliferative activated receptor, gamma | PPARG | 2.28 | 1.47 | 3p25 | LH/IR |
| 209398_at | histone 1, H1c | HIST1H1C | -3.13 | -2.38 | 6p21.3 | |
| 214290_s_at | histone 2, H2aa | H2AFO | -5.56 | -4.61 | 1q21.2 | |
| 218280_x_at | histone 2, H2aa | HIST2H2AA | -3.25 | -2.76 | 1q21.2 | |
| 221582_at | histone 3, H2a | HIST3H2A | -2.46 | -1.13 | 1q42.13 | |
| 215071_s_at | histone 1, H2ac | HFE | -2.45 | -1.51 | 6p21.3 | |
| 222067_x_at | histone 1, H2bd | HFE | -3.86 | -2.36 | 6p21.3 | |
| 209911_x_at | histone 1, H2bd | HIST1H2BD | -2.37 | -1.81 | 6p21.3 | |
| 202708_s_at | histone 2, H2be | HIST2H2BE | -2.32 | -2.55 | 1q21-q23 | |
| Immune respons | | | | | | |
| 214677_x_at | immunoglobulin lambda joining 3 | IGLJ3 | -12.88 | -2.57 | 22q11.1-q11.2 | IM |
| 209138_x_at | immunoglobulin lambda joining 3 | IGLJ3 | -7.13 | -2.27 | 22q11.1-q11.2 | IM |
| 215121_x_at | immunoglobulin lambda joining 3 | IGLJ3 | -3.99 | -1.92 | 22q11.1-q11.2 | IM |
| 215379_x_at | immunoglobulin lambda joining 3 | IGLJ3 | -5.08 | -1.98 | 22q11.1-q11.2 | IM |
| 221671_x_at | immunoglobulin kappa constant | IGKC | -11.78 | -5.11 | 2p12 | IM |
| 217478_s_at | major histocompatibility complex, class II, DM alpha | HLA-DMA | -2.11 | -1.61 | 6p21.3 | IM |
| 203932_at | major histocompatibility complex, class II, DM beta | HLA-DMB | -2.07 | -1.41 | 6p21.3 | IM |
| 211991_s_at | major histocompatibility complex, class II, DP alpha 1 | HLA-DPA1 | -2.37 | -1.35 | 6p21.3 | IM |
| 212671_s_at | major histocompatibility complex, class II, DQ alpha 1 | HLA-DQA1 | -8.35 | -1.67 | 6p21.3 | IM |
| 211656_x_at | major histocompatibility complex, class II, DQ beta 1 | HLA-DQB1 | -2.98 | -1.78 | 6p21.3 | IM |

Table 1. Continued

| | | | | | | |
|---|---|---------------|-------|-------|---------------|----------|
| 210982_s_at | major histocompatibility complex, class II, DR alpha | HLA-DRA | -9.66 | -1.53 | 6p21.3 | IM |
| 208894_at | major histocompatibility complex, class II, DR alpha | HLA-DRA | -3.48 | -1.55 | 6p21.3 | IM |
| 209312_x_at | major histocompatibility complex, class II, DR beta 1 | HLA-DRB1 | -2.54 | -1.62 | 6p21.3 | IM |
| 204670_x_at | major histocompatibility complex, class II, DR beta 5 | HLA-DRB5 | -3.41 | -2.8 | 6p21.3 | IM |
| 209619_at | CD74 antigen (invariant polypeptide of major histocompatibility complex class II) | CD74 | -1.94 | -1.56 | 5q32 | IM |
| 227697_at | suppressor of cytokine signaling 3 | SSI-3 | -6.62 | -6.7 | 17q25.3 | IM/AP |
| 217767_at | complement component 3 | C3 | -6.05 | -2.28 | 19p13.3-p13.2 | IM |
| 211796_s_at | T cell receptor beta locus | TRB@ | -5.11 | -1.37 | 7q34 | IM |
| 210915_x_at | T cell receptor beta locus | TRB@ | -2.35 | -1.38 | 7q34 | IM |
| 208078_s_at | transcription factor 8 (represses interleukin 2 expression) | TCF8 | -4.25 | -4.02 | 10p11.2 | IM |
| 205114_s_at | chemokine (C-C motif) ligand 3 | CCL3 | -3.24 | -2.33 | 17q11-q21 | IM |
| Extracellular Matrix | | | | | | |
| 222486_s_at | a disintegrin-like and metalloprotease (repolysin type) with thrombospondin type 1 motifs | ADAMTS1 | -4.51 | -3.04 | 21q21.2 | EC/LH/CL |
| 222162_s_at | a disintegrin-like and metalloprotease (repolysin type) with thrombospondin type 1 motifs | ADAMTS1 | -2.6 | -2.37 | 21q21.2 | EC/LH/CL |
| 202994_s_at | fibulin 1 | FBLN1 | -3.51 | 1.03 | 22q13.31 | EC |
| 201787_at | fibulin 1 | FBLN1 | -3.27 | -1.37 | 22q13.31 | EC |
| 202995_s_at | fibulin 1 | FBLN1 | -1.87 | -1.16 | 22q13.31 | EC |
| 213992_at | collagen, type IV, alpha 6 | COL4A6 | -2.2 | -1.38 | Xq22 | EC |
| 213905_x_at | biglycan | BGN | 1.82 | -1.01 | Xq28 | EC |
| 201262_s_at | biglycan | BGN | 3.09 | 1.11 | Xq28 | EC |
| 205907_s_at | osteomodulin | OMD | 2.14 | 2.19 | 9q22.1 | EC |
| 205908_s_at | osteomodulin | OMD | 2.71 | 2.8 | 9q22.1 | EC |
| 204114_at | nidogen 2 (osteonidogen) | NID2 | 1.95 | 1.29 | 14q21-q22 | EC |
| 201109_s_at | thrombospondin 1 | THBS1 | 2.26 | 1.41 | 15q15 | EC |
| 205465_x_at | heparan sulfate (glucosamine) 3-O-sulfotransferase 1 | HS3ST1 | 2.41 | 1.2 | 4p16 | EC |
| 206233_at | UDP-Gal:beta-GlcNAc beta 1,4- galactosyltransferase, polypeptide chain B | B4GALT6 | 2.68 | 1.95 | 18q11 | EC |
| 205114_s_at | a disintegrin and metalloproteinase domain 12 (meltrin alpha) | ADAM12 | 2.21 | 1.91 | 10q26.3 | EC |
| Membrane receptors/Associated proteins/solute carriers | | | | | | |
| 206812_at | adrenergic, beta-3-, receptor | ADRB3 | -2.58 | -1.63 | 8p12-p11.2 | |
| 227556_at | ATPase, Na+/K+ transporting, beta 1 polypeptide | ATP1B1 | -2.5 | -1.74 | 1q22-q25 | |
| 226695_at | progesterone receptor membrane component 2 | PGRMC2 | -3.93 | -1.2 | 4q26 | |
| 219423_x_at | tumor necrosis factor receptor superfamily, member 25 | TNFRSF25 | 1.96 | 1.34 | 1p36.2 | |
| 208868_s_at | GABA(A) receptor-associated protein like 1 | GABARAPL1 | -1.98 | -1.17 | 12p13.31 | |
| 202088_at | complement component 5 receptor 1 (C5a ligand) | C5R1 | -1.86 | -2.04 | 19q13.3-q13.4 | IM |
| 226709_at | roundabout, axon guidance receptor, homolog 2 (Drosophila) | ROBO2 | 1.86 | 1.25 | 3p12.3 | |
| 219090_at | solute carrier family 24 (sodium/potassium/calcium exchanger), member 3 | SLC24A3 | -6.34 | 1.35 | 20p13 | |
| 202499_s_at | solute carrier family 2 (facilitated glucose transporter), member 3 | SLC2A3 | -2.54 | -2.55 | 12p13.3 | |
| 216092_s_at | solute carrier family 7 (cationic amino acid transporter, y+ system) | SLC7A8 | -1.81 | -1.84 | 14q11.2 | |
| 219229_at | solute carrier family 21 (organic anion transporter), member 11 | SLC21A11 | 1.85 | 1.4 | 15q26 | |
| 205857_at | solute carrier family 18 (vesicular monoamine), member 2 | SLC18A2 | 2.28 | 1.59 | 10q25 | |
| Miscellaneous | | | | | | |
| 202284_s_at | cyclin-dependent kinase inhibitor 1A (p21, Cip1) | CDKN1A | -4.45 | -2.94 | 6p21.2 | CL |
| 207016_s_at | aldehyde dehydrogenase 1 family, member A2 | ALDH1A2 | -4.41 | -1.21 | 15q21.2 | RA |
| 203649_s_at | phospholipase A2, group IIA (platelets, synovial fluid) | PLA2G2A | -7.11 | -2.31 | 1p35 | |
| 209278_s_at | tissue factor pathway inhibitor 2 | TFPI2 | -4.21 | -1.14 | 7q22 | |
| 202388_at | regulator of G-protein signalling 2, 24kDa | RGS2 | -4.03 | -1.69 | 1q31 | LH |
| 225557_at | AXIN1 up-regulated | AXUD1 | -3.78 | -4.06 | 3p22 | |
| 202437_s_at | cytochrome P450, family 1, subfamily B, polypeptide 1 | CYP1B1 | -3.71 | -1.5 | 2p21 | |
| 203662_s_at | tropomodulin | TMOD | -3.49 | -1.15 | 9q22.3 | |
| 213013_at | mitogen-activated protein kinase 8 interacting protein 1 | MAPK8IP1 | -3.28 | -1.85 | 11p12-p11.2 | MK |
| 227758_at | RAS-like, estrogen-regulated, growth-inhibitor | RERG | -3.24 | -1.55 | 12p13.1 | |
| 209792_s_at | kallikrein 10 | KLK10 | -3.24 | -1.48 | 19q13.3-q13.4 | |
| 223218_s_at | molecule possessing ankyrin repeats induced by lipopolysaccharide | MAIL | -3.12 | -2.65 | 3p12-q12 | |
| 36711_at | v-maf musculoaponeurotic fibrosarcoma oncogene homolog F (avian) | MAFF | -2.87 | -2.33 | 22q13.1 | |
| 201288_at | Rho GDP dissociation inhibitor (GDI) beta | ARHGDIB | -2.84 | -1.3 | 12p12.3 | |
| 218345_at | hepatocellular carcinoma-associated antigen 112 | HCA112 | -2.64 | -2.22 | 7q36.1 | |
| 203186_s_at | S100 calcium binding protein A4 (calcium protein, calyculin, me) | S100A4 | -2.37 | -1.44 | 1q21 | |
| 209596_at | adican | DKFZp564i1922 | -2.37 | -1.41 | Xp22.33 | |
| 204472_at | GTP binding protein overexpressed in skeletal muscle | GEM | -2.34 | -1.53 | 8q13-q21 | |
| 210715_s_at | serine protease inhibitor, Kunitz type, 2 | SPINT2 | -2.34 | -1.5 | 19q13.1 | |
| 215785_s_at | cytoplasmic FMRP interacting protein 2 | CYFIP2 | -2.28 | -1.56 | 5q34 | |
| 202376_at | serine (or cysteine) proteinase inhibitor, clade A (alpha-1 antitrypsin) | SERPINA3 | -2.28 | -1.15 | 14q32.1 | |
| 209897_s_at | slit homolog 2 (Drosophila) | SLIT2 | -2.26 | -1.25 | 4p15.2 | |
| 204916_at | receptor (calcitonin) activity modifying protein 1 | RAMP1 | -2.21 | -1.31 | 2q36-q37.1 | |
| 212099_at | ras homolog gene family, member B | ARHB | -2.11 | -2.98 | 2p24.1 | |
| 225177_at | Rab coupling protein | RCP | -2.07 | -1.75 | 8p11.22 | |
| 209277_at | tissue factor pathway inhibitor 2 | TFPI2 | -2.06 | -1.06 | 7q22 | |
| 209613_s_at | alcohol dehydrogenase IB (class I), beta polypeptide | ADH1B | -2.02 | 1.07 | 4q21-q23 | |
| 223169_s_at | Wnt-1 responsive Cdc42 homolog | ARHU | -1.89 | -1.23 | 1q42.11-q42.3 | WN |
| 214247_s_at | dickkopf homolog 3 (Xenopus laevis) | DKK3 | 1.8 | 1.58 | 11p15.2 | WN |
| 205990_s_at | wingless-type MMTV integration site family, member 5A | WNT5A | 1.97 | 1.12 | 3p21-p14 | WN |
| 210740_s_at | inositol 1,3,4-triphosphate 5/6 kinase | ITPK1 | -1.88 | -1.39 | 14q31 | |
| 218501_at | Rho guanine nucleotide exchange factor (GEF) 3 | ARHGEF3 | -1.84 | -1.42 | 3p21-p13 | |
| 211373_s_at | presenilin 2 (Alzheimer disease 4) | PSEN2 | -1.82 | -1.26 | 1q31-q42 | |
| 222719_s_at | platelet derived growth factor C | PDGFC | 1.82 | 1.4 | 4q32 | |
| 221898_at | lung type-I cell membrane-associated glycoprotein | T1A-2 | 1.82 | 1.47 | 1p36 | |
| 206176_at | bone morphogenetic protein 6 | BMP6 | 1.88 | 1.19 | 6p24-p23 | |
| 218730_s_at | osteoglycin (osteoinductive factor, mimecan) | OGN | 1.92 | 1.28 | 9q22 | |
| 225977_at | protocadherin 18 | PCDH18 | 1.92 | 1.57 | 4 | |
| 201909_at | ribosomal protein S4, Y-linked | RPS4Y | 1.94 | 1.04 | Yp11.3 | |
| 203999_at | synaptotagmin I | SYT1 | 1.94 | 1.39 | 12cen-q21 | |

Table 1. Continued

| | | | | | |
|----------------------|--|-------------|--------|--------------|--------------|
| 201860_s_at | plasminogen activator, tissue | PLAT | 1.98 | 1.03 | 8p12 |
| 203130_s_at | kinesin family member 5C | KIF5C | 2.08 | 1.53 | 2q23.3 |
| 204450_x_at | apolipoprotein A-I | APOA1 | 2.15 | 1.46 | 11q23-q24 |
| 226766_at | roundabout, axon guidance receptor, homolog 2 (Drosophila) | ROBO2 | 2.22 | 1.29 | 3p12.3 |
| 226618_at | ankyrin 3, node of Ranvier (ankyrin G) | SOAT1 | 2.22 | 1.81 | 10q21 |
| 225626_at | phosphoprotein associated with glycosphingolipid-enriched micro- | PAG | 2.23 | 1.05 | 8q21.11 |
| 208664_s_at | tetratricopeptide repeat domain 3 | TTC3 | 2.25 | 2.61 | 21q22.2 |
| 215983_s_at | reproduction 8 | D8S2298E | 2.3 | 1.59 | 8p12-p11.2 |
| 229704_at | androgen-induced proliferation inhibitor | AS3 | 2.51 | 1.19 | 13q12.3 |
| 210424_s_at | golgin-67 | GOLGIN-67 | 2.66 | 2.03 | 15q11.2 |
| ESTs/ unknown | | | | | |
| 229947_at | ESTs | 229947_at | -11.53 | -1.73 | 7q21.11 |
| 242836_at | ESTs | 242836_at | -6.98 | -5.01 | 3q23 |
| 224559_at | Homo sapiens clone alpha1 mRNA sequence | 224559_at | -4.13 | -3.55 | 11q13.1 |
| 225996_at | | 225996_at | -3.02 | -1.98 | 2q11.2 |
| 227337_at | hypothetical protein FLJ11200 | FLJ11200 | -2.71 | -2.33 | 4q35.1 |
| 241358_at | ESTs | 241358_at | -2.58 | -1.46 | 17q21.33 |
| 229189_s_at | hypothetical protein BC006130 | LOC93622 | -2.57 | -1.27 | 4p16.1 |
| 226552_at | ESTs | 226552_at | -2.46 | -2.3 | 9q12 |
| 228325_at | KIAA0146 protein | KIAA0146 | -2.41 | -2.65 | 8q11.21 |
| 241824_at | ESTs | 241824_at | -2.36 | -1.61 | 2p23.2 |
| 219144_at | hypothetical protein MGC1136 | MGC1136 | -2.36 | 1.04 | 8p11.23 |
| 227099_s_at | Homo sapiens, clone IMAGE:4944483, mRNA | 227099_s_at | -2.3 | -1.92 | 11p11.2 |
| 222150_s_at | hypothetical protein LOC54103 | LOC54103 | -2.25 | -1.3 | 7q11.23 |
| 213142_x_at | hypothetical protein LOC54103 | LOC54103 | -2.18 | -1.32 | 7q11.23 |
| 201141_at | glycoprotein (transmembrane) nmb | GNPMB | -2.13 | -1.19 | 7p15 |
| 235317_at | Homo sapiens mRNA | 235317_at | -2.07 | -1.85 | 19p13.13 |
| 232139_s_at | KIAA1919 protein | KIAA1919 | -2.07 | -1.65 | 6q21 |
| 227613_at | Homo sapiens full length insert cDNA clone YZ93G08 | 227613_at | -2.05 | -1.64 | 19q13.41 |
| 226811_at | retinoblastoma binding protein 7 | FLJ20202 | -2.01 | -1.04 | 1p11.1 |
| 222801_s_at | hypothetical protein FLJ13195 similar to stromal antigen 3 | FLJ13195 | -2 | -1.07 | 7p11.2-q11.2 |
| 226435_at | | MGC50452 | -1.99 | -1.02 | 14q24.2 |
| 233121_at | --- | 233121_at | -1.96 | -1.06 | 8q24.13 |
| 227163_at | --- | bA127L20.1 | -1.95 | -1.08 | 10q25.1 |
| 238028_at | Homo sapiens cDNA FLJ90086 fis, clone HEMBA1005145. | 238028_at | -1.91 | -1.49 | 6p21.1 |
| 228896_at | ESTs, Weakly similar to hypothetical protein FLJ10330 [Homo se | 228896_at | -1.91 | -1.08 | 3p22.3 |
| 224990_at | hypothetical protein LOC201895 | LOC201895 | -1.9 | -1.26 | 4p14 |
| 229082_at | ESTs, Weakly similar to hypothetical protein FLJ20294 [Homo se | 229082_at | -1.88 | -1.66 | 5q15 |
| 223299_at | similar to signal peptidase complex (18kD) | LOC90701 | -1.87 | -1.65 | 18q21.31 |
| 223411_at | AD023 protein | AD023 | -1.85 | -1.35 | 17q25.2 |
| 224579_at | Homo sapiens cDNA FLJ14201 fis, clone NT2RP3002955. | 224579_at | -1.84 | -1.19 | 12q13.11 |
| 227297_at | Homo sapiens cDNA: FLJ23173 fis, clone LNG10019. | 227297_at | 1.8 | 1.21 | 3p22.3 |
| 236576_at | ESTs | 236576_at | 1.8 | 1.42 | 10q21.3 |
| 243416_at | ESTs | 243416_at | 1.82 | 1.6 | 1p31.3 |
| 227198_at | Homo sapiens cDNA FLJ30555 fis, clone BRAWH2003818. | 227198_at | 1.84 | 1.37 | 2q11.2 |
| 229802_at | Homo sapiens cDNA FLJ14388 fis, clone HEMBA1002716. | 229802_at | 1.85 | -1.14 | 8q24.22 |
| 232174_at | Homo sapiens clone 24838 mRNA sequence | 232174_at | 1.85 | 1.34 | 8q24.11 |
| 225382_at | | psHMG17 | 1.91 | 1.12 | Xq28 |
| 213381_at | | 213381_at | 1.93 | 1.56 | 10q11.23 |
| 232458_at | Homo sapiens cDNA FLJ11469 fis, clone HEMBA1001658. | 232458_at | 1.81 | 1.61 | 2q32.2 |
| 226997_at | Homo sapiens cDNA FLJ10196 fis, clone HEMBA1004776. | 226997_at | 1.82 | 1.16 | 5p13.3 |
| 202771_at | KIAA0233 gene product | KIAA0233 | 1.94 | -1.05 | 16q24.3 |
| 226726_at | hypothetical protein BC016005 | LOC129642 | 1.95 | 1.82 | 2p25.2 |
| 242396_at | Homo sapiens cDNA FLJ10010 fis, clone HEMBA1000302. | 242396_at | 2.02 | 2.06 | 15q26.2 |
| 230617_at | ESTs | 230617_at | 2.03 | -1.42 | 11q13.1 |
| 226612_at | Homo sapiens cDNA FLJ25076 fis, clone CBL06117. | SOAT1 | 2.05 | 2.01 | 5p15.31 |
| 230061_at | hypothetical protein BC014339 | LOC116441 | 2.09 | 1.54 | 3q24 |
| 209286_at | Homo sapiens cDNA FLJ31353 fis, clone MESAN2000264. | CEP3 | 2.09 | 2.17 | 2p22.2 |
| 231980_at | | 231980_at | 2.11 | 1.35 | 18q22.2 |
| 244057_s_at | Homo sapiens mRNA | 244057_s_at | 2.14 | 1.75 | 10q11.23 |
| 213790_at | Homo sapiens cDNA FLJ31066 fis, clone HSYRA2001153. | ADAM12 | 2.21 | 2.1 | 10q26.3 |
| 241560_at | ESTs | 241560_at | 2.25 | 1.81 | 4q27 |
| 215555_at | hypothetical protein LOC148936 | LOC148936 | 2.36 | 1.88 | 1p36.11 |
| 230311_s_at | | PRDM6 | 2.58 | 1.96 | 5q23.2 |
| 228653_at | ESTs, Weakly similar to hypothetical protein FLJ20489 [Homo se | 228653_at | 3.67 | 1.19 | 6q24.3 |
| 219463_at | chromosome 20 open reading frame 103 | C20orf103 | 4.02 | 3.44 | 20p12 |

Sequence codes are the Affymetrix probe identifiers. Annotations are derived from Affymetrix and additional features are available at the NetAffx analysis center (<http://www.affymetrix.com/analysis/index.affx>). FC, Fold change; N, normal; MK, linked with MAPK signaling pathways; LH, expression regulated by LH; IM, immunological component; PR, associated with proliferation-regulated pathways; SR, stress response; AP, apoptosis; EC, extracellular matrix; CL, expression linked with corpus luteum formation or luteolysis; RA, retinoic acid synthesis pathway; IR, insulin resistance linked; WN, Wnt-signaling pathway.

ing PCOS and normal ovary samples. Furthermore, the present analysis revealed up- and down-regulated genes associated with cell proliferation and LH-regu-

lated periovulatory processes. This is not unexpected because the arrest in follicle development induces an anovulatory state as can be encountered in PCOS

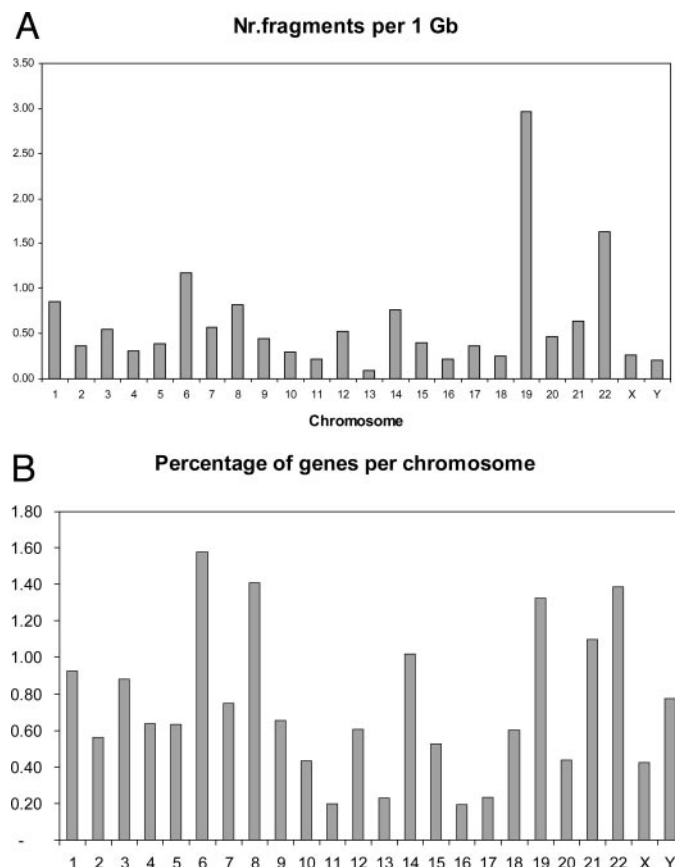


Fig. 3. Chromosomal Mapping of Genes with Altered Expression in PCOS Ovaries

The number of genes with differential expression in PCOS is expressed per gigabase pairs of chromosome size (A), or as the percentage of the total number of genes mapped on the respective chromosome (B). The chromosomal content data were obtained from the Ensembl genome data resources (www.ensembl.org) using Human Genome Browser release 17.33.1.

ovaries. Some of these genes and their role in ovarian function, such as NGFI-B (32), C/EBP β (33), p21Cip (34), and SGK (35), have been described previously. However, some of the identified genes are novel and their potential role in human folliculogenesis remains to be determined. Finally, our results demonstrate that the majority of regulated genes display differential expression in both PCOS and TSX ovaries, providing additional support for hyperandrogenemia being the central mechanism underlying PCOS. It should be noted that some reservation regarding the interpretation of these results seems justified at this stage, because the exact nature and cellular content of the ovarian biopsies remain unknown. For instance, the possibility of relative differences in stromal content comparing PCOS, TSX, and control tissue cannot be excluded.

The present study shows that the majority of the differentially expressed genes are down-regulated in PCOS ovaries, suggesting that several processes that are activated by these genes are in a “off-state.” This may not be surprising because it is consistent with a less active state of PCOS ovaries with respect to the later follicular stages (*i.e.* dominant and preovulatory) as compared with controls. Accordingly, we identified

several down-regulated genes from which it is well established that they are either induced by LH, or their expression levels are elevated in the post-LH surge and/or periovulatory window. These represent markers such as C/EBP β , EGR-1, NGFI-B, Jun D, and ADAMTS-1. Their relative underexpression is in accordance with the absence of ovulation in PCOS. Remarkably, androgen-regulated genes such as Pem (37) and OTEX (38) were not differentially expressed in the present study. This might be explained by a stable status of PCO, exposed to elevated androgen levels for an extended period of time. Such a condition could result in a decline of the androgen response at the level of gene transcription. Again, the possibility cannot be excluded that observed differences might be due to differences in cell populations studied, because the present samples constitute a mixture of follicular (theca, granulosa, oocyte) and stromal components. For example, the selection of ECM genes that we identified as being differentially expressed may result from genes expressed in the stromal/epithelial compartment and therefore might not be differentially expressed in the *in vitro* theca cell cultures. Finally, theca cells might behave differently *in vitro* compared with

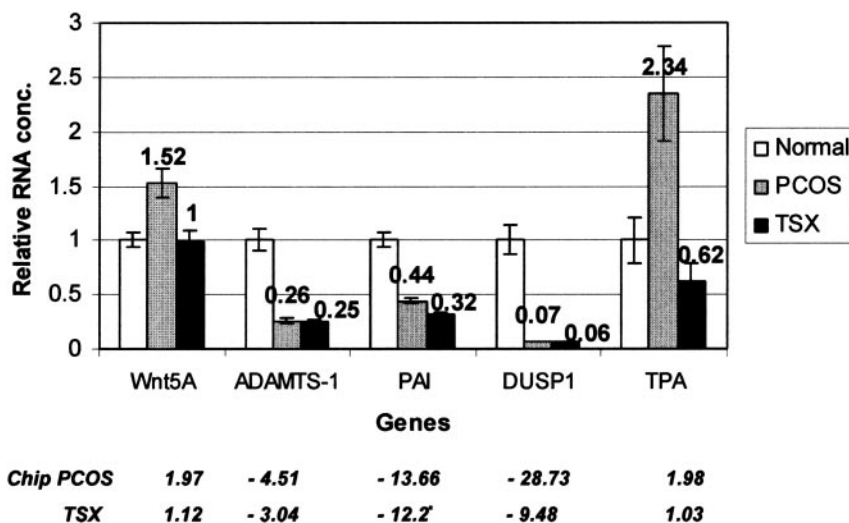


Fig. 4. Comparison of Gene Expression in Microarray Analysis with Real-Time Q-PCR Analysis

Relative mRNA levels as identified by microarray analysis of PCOS, TSX, and control ovary samples are compared with the differential expression as determined in Q-PCR experiments. *, $P = 0.03$; Wnt5A, wingless-type murine mammary tumor virus (MMTV) integration site family member 5A; PAI, plasminogen activator inhibitor; TPA, tissue plasminogen activator (PLAT).

the *in vivo* situation in which they are embedded and among other endocrine cells.

By comparing the transcriptome of PCOS ovaries and normal ovaries, we set out to identify gene networks and signal transduction pathways that are abnormal in PCOS. These deviant pathways may play important roles in arrested follicle development and hence represent a key feature of the PCOS phenotype. This approach might lead to a series of candidate genes, which might subsequently be evaluated and validated using other genetic approaches. When browsing the table of genes with altered expression in PCOS ovaries, several aberrant pathways can be identified, and these are discussed below.

Wnt Signaling

At least four genes that are linked to Wnt signaling show altered expression in PCOS: 1) Wnt-1-responsive Cdc42 homolog (up); 2) dickkopf homolog 3 (down); 3) Wnt5A (up); and 4) carboxypeptidase Z (up). Moreover, dickkopf is a Wnt signaling inhibitor (39), and very recently it has been shown that carboxypeptidase Z also inhibits Wnt signaling (40). The spatial and temporal distribution of activating and inhibitory factors determines whether Wnt signaling is activated or repressed in PCOS ovaries. In a recent microarray study using theca cells from PCOS and controls, Wnt signaling was also shown to be altered (13). Moreover, several reports demonstrate that Wnt signaling factors are expressed and hormonally regulated in the adult rat ovary (36, 41, 42).

ECM Components and ECM Remodeling Factors

At least 10 genes that are linked to the ECM are differentially expressed in PCOS: fibulin 1; biglycan;

nidogen 2; thrombospondin 1 (THBS1); a disintegrin and metalloprotease with thrombospondin motifs-1 (ADAMTS1); heparan sulfate (glucosamine) 3-O-sulfotransferase 1; UDP-Gal:βGlcNAc β 1,4-galactosyltransferase, polypeptide 6 (B4GALT6); osteomodulin; collagen type IV and ADAM12. Nidogen 2 is a potential ligand of fibulin 1 (43). All factors, except fibulin, ADAMTS1, and collagen type IV are up-regulated in PCOS ovaries. In TSX ovaries, only B4GALT6, osteomodulin, and ADAM12 are up-regulated. It is tempting to speculate that the altered expression of these genes in PCOS is related to the process of cyst formation and/or physical properties of the thick ovarian capsule. In addition, THBS1 expression is associated with local neovascularization processes in the ovary and its expression is high in early antral follicles. An increased amount of these follicles is present in PCOS ovaries compared with controls (10, 11).

Immune System Components

At least 17 genes that are linked to the immune system show altered expression in PCOS: Ig λ joining 3; Ig κ constant; major histocompatibility complex (MHC), class II, DRα; MHC class II, DP α 1; MHC class II, DR β 1 and 5; MHC class II, DQ α 1; MHC class II, DQ β 1; MHC class II, DM β; MHC class II, DM α; CD74; T cell receptor β locus; complement component C3; suppressor of cytokine signaling 3; transcription factor 8; chemokine ligand 3. All factors are expressed at a lower mRNA level in PCOS ovaries. TSX ovaries display a similar profile, although all but one of the MHC genes are not regulated. It has become apparent that in the ovary the immune system contributes to the regulation of gonadal function (44, 45). Immune cells are not detectable in the granulosa layer until the LH

surge occurs. MHC class II DR is highly expressed in human large luteinized cells (46). It has been proposed that luteinized cells communicate with T cells during formation and subsequent demise of the corpus luteum. Moreover, the actual rupture process of the follicle displays characteristics of an inflammatory reaction. In addition, it has been shown that MHC class II molecules (e.g. HLA DR) are expressed by granulosa cells after luteal transformation (47–49). The observed lower expression of these immune system components in PCOS and TSX ovaries relates to the fact that these periovulatory processes are almost absent in ovaries of PCOS patients.

Apoptosis and Stress Response

A large number of genes that have a lower expression in both PCOS and TSX ovaries are positive regulators of cell proliferation. We identified the phosphatase DUSP1 (dual specificity phosphatase 1) as being strongly down-regulated in PCOS ovaries as well as TSX ovaries. This DUSP1 expression profile is comparable to what has been published on NGFI-B displaying a rapid and transient stimulation by human chorionic gonadotropin (32). The downstream substrates of DUSP1 are members of p38 MAPK, the Erk and c-Jun N-terminal kinase pathways. Because these are inactivated by the phosphatase activity of DUSP1, the reduced DUSP1 mRNA levels in PCOS ovaries might therefore (transiently) activate p38MAPK, Erk, and c-Jun N-terminal kinase signaling. Activation of these pathways is required to mediate apoptosis induced by proinflammatory cytokines such as TNF (50). Interestingly, TNFRSF25, a member of the TNF receptor superfamily involved in inducing apoptosis (51), is expressed at a higher level in PCOS ovaries.

Heat Shock Proteins (HSPs)

Five genes encoding heat shock proteins are expressed at a reduced level in PCOS: DnaJ (HSP40) homolog, subfamily B, member 1; heat shock 70-kDa protein 6 (HSP70B); heat shock 70-kDa protein 1A; heat shock 70-kDa protein 1B; and heat shock 90-kDa protein 1 α . The 70-kDa stress protein family (HSP70) plays important roles in a variety of physiological processes, including protein chaperoning, steroidogenesis, and protection against apoptosis and is a general mediator of cellular stress responses. In summary, some apoptotic processes might be activated in PCOS ovaries as compared with controls. Indeed it has been suggested that the number of atretic follicles is increased in PCOS patients (52). In addition, induction of HSP70 is associated with inhibition of hormone-sensitive, LH-induced steroidogenesis via inhibition of steroid acute regulatory protein synthesis. The down-regulated HSP70 in PCOS therefore does not interfere with steroid synthesis. This is consistent with the observation that androgenic steroid produc-

tion is even higher in PCOS as compared with control individuals (12).

Peroxisome Proliferator-Activated Receptor (PPAR) γ and Histone Deacetylase 3 (HDAC3) in Proliferation/Differentiation

HDAC3 has an important function in regulating PPAR γ activity (53). HDAC inhibition is more effective in suppressing growth and inducing differentiation when treatment is combined with PPAR γ agonists. Actually, in PCOS ovaries we identified HDAC3 as down-regulated and PPAR γ as up-regulated. This might result in locally enhanced differentiation-promoting activity in PCOS ovaries and may be involved in the process of follicle arrest in PCOS. Expression of both genes is not altered in TSX. In this context it is important to note that a commonly used antiepileptic drug, valproic acid (VPA), has both HDAC-inhibitory activity and agonistic activity on PPAR γ (54, 55). Interestingly, VPA treatment is associated with PCOS-like features because these patients develop hyperandrogenism and PCO during VPA treatment (56, 57). Moreover, VPA does increase androgen synthesis in ovarian theca cells (58). Finally, PCOS-like features disappear when VPA therapy is discontinued. In addition, two independent studies show that polymorphism in the PPAR γ gene might be associated with PCOS (59–61).

Until now the etiology of PCOS remains unknown. When the differentially regulated genes in PCOS and TSX are analyzed for their chromosomal location, it becomes apparent that chromosome 19 displays the highest relative score. This is intriguing, because several studies provide support for a genetic basis for PCOS (62, 63) and demonstrated linkage to chromosome 19p13.3. Our microarray experiments revealed two genes that are located in this chromosomal interval: complement component 3 and growth arrest and DNA damage-inducible β (GADD45B). However, we do not yet have functional links that associate one of these genes with PCOS. The identification of pathways that are abnormal in PCOS may contribute to understanding the pathophysiology of PCOS and the identification of causative molecular factors and therefore might reveal novel leads for therapeutic intervention.

MATERIALS AND METHODS

Subjects

This study was approved by the institutional ethical review boards of Erasmus Medical Center, the Daniel den Hoed Oncology Hospital (both located in Rotterdam), as well as the Flevo Hospital in Almere, The Netherlands. Participants were recruited from all three aforementioned hospitals. All subjects had undergone surgery during the period 1998–2002. Written informed consent was obtained from all participants.

In normoovulatory controls uni- or bilateral oophorectomy was performed because subjects were either carriers of a known gene mutation (BRCA 1 or 2) or their family history

indicated a severely increased chance of ovarian cancer (64) or because of other gynecological conditions. Only women with regular menstrual cycles (21–35 d) and younger than 40 yr were included in this study. The BMI (kg/m^2) was recorded in all patients. Women with PCO, defined as more than 12 follicles smaller than 10 mm present in at least one ovary, detected by ultrasound, were excluded. Similarly, if ovarian cancer was shown to be present in one or both ovaries, patients were excluded.

Women between 20 and 40 yr of age and having PCOS were recruited from the infertility clinic of the Erasmus Medical Center. PCOS was defined according to the latest PCOS consensus (1, 2). Briefly, women should have irregular menstrual cycles and/or clinical or endocrine hyperandrogenism [$\text{FAI} (\text{T} \times 100/\text{sex hormone binding globulin (SHBG)}) > 4.5$] and/or PCO on ultrasound. All patients with at least two of the four aforementioned criteria were considered to have PCOS and were included. All patients had a long standing history of infertility, and all underwent ovulation induction without achieving a pregnancy. All patients previously developed moderate to severe ovarian hyperstimulation syndrome. In all PCOS patients uni- or bilateral ovarian biopsies were performed.

TSX individuals underwent hysterectomy and bilateral oophorectomy because of their sex reversal. Only subjects aged between 20 and 40 yr with a history of regular menstrual cycles (21–35 d) and without a previous history of hyperandrogenemia were included. In all TSX subjects, 250 μg T (Sustanon, Organon, Oss, The Netherlands) had been administered im once biweekly during at least half a year before surgery was performed.

Interventions

Standardized initial screening (clinical investigation, transvaginal ultrasound, and fasting blood withdrawal) was performed between 0900–1100 h, as previously described (65). For sonographic imaging we used a 6.5-MHz vaginal transducer (model EUB-415, Hitachi Medical Corp., Tokyo, Japan). The ovaries were localized and scanned as described previously (65). Ultrasonography as well as endocrinological screening was only performed in PCOS patients and TSX individuals. In PCOS patients blood withdrawal was performed on a random day. In TSX individuals blood was withdrawn before T treatment was initiated.

Bilateral oophorectomy in normoovulatory controls was performed laparoscopically under general anesthesia. Each ovary was removed using ultrasonic scissors. After cutting the suspending ligaments, one ovary was removed from the peritoneal cavity through a small incision in the lateral abdominal wall. The remaining ovary was thereafter removed by a similar procedure. In TSX individuals oophorectomy was performed either via the abdominal or vaginal route using standard gynecological techniques. Ovarian biopsies from both ovaries were taken in PCOS patients during laparoscopy. Biopsies constituted minimal wedges taken at the equatorial plane at the antimesovarian edge of each ovary. Care was taken that both cortical and stroma components were collected. Generally, biopsies constituted about one tenth of each ovary and had a pyramidal shape with the top of the pyramid being located at the ovarian hilus. Hemostasis was achieved using bipolar scissors. All tissue samples were processed immediately after collection. Biopsies were snap frozen in liquid nitrogen immediately after collection, whereas whole ovaries were cut in quarters. A randomly selected quarter was subsequently snap frozen. Sections for the remaining tissue samples were histologically processed and microscopically evaluated according to standard procedures (30).

Hormone Assays

Blood samples were obtained by venapuncture and processed within 2 h after withdrawal. Serum was stored at -20°C and assayed for LH, FSH, androstenedione (AD), T, SHBG, dehydroepiandrosterone (DHEA), dehydroepiandrosterone sulfate (DHEAS), and E_2 . Serum levels of LH, FSH, and SHBG were assessed using luminescence-based immunoassays (Immulin, Diagnostic Products Corp., Los Angeles, CA), whereas serum E_2 , T, AD, DHEA, and DHEAS levels were measured using coated tube RIAs provided by the same supplier. Intra- and interassay coefficients of variation were less than 5% and 15% for LH, less than 3% and 8% for FSH, less than 8% and 11% for AD, less than 3% and 6% for DHEA and DHEAS, less than 3% and 5% for T, less than 5% and 7% for E_2 , and less than 4% and 5% for SHBG, respectively.

RNA Sample Preparation

Total RNA was extracted from the biopsies using TRIZOL reagent (Invitrogen, Breda, The Netherlands) as per the manufacturer's instructions. After TRIZOL purification, RNA was repurified using the RNeasy Mini Kit (QIAGEN, Venlo, The Netherlands) according to the manufacturer's protocol. Total RNA was quantified by $\text{OD}_{260}/\text{OD}_{280}$ measurement and with the RiboGreen RNA Quantitation Kit (Molecular Probes, Leiden, The Netherlands). RNA quality was assessed on a 6000 nanochip using the Agilent 2100 bioanalyzer (Agilent Technologies, Waldbronn, Germany).

cDNA Synthesis and Q-PCR

To 1 μg total RNA comprising a pooled sample (either PCOS, TSX, or normal), 0.5 μg Oligo(dT)15 primer (Promega, Leusden, The Netherlands) and 1 μg random hexamers pd(N)₆ (Amersham Biosciences, Roosendaal, The Netherlands) were added in a total volume of 12 μl . The mixture was heated at 70°C for 10 min and quickly chilled on ice for 5 min. cDNA was synthesized in a total volume of 20 μl containing 50 mM Tris-HCl (pH 8.3), 75 mM KCl, 3 mM MgCl_2 , 10 mM dithiothreitol, 0.5 mM deoxynucleotide triphosphates and 200 U Superscript II RNase H⁻ Reverse Transcriptase (Invitrogen). After incubation for 1 h at 37°C , the enzyme was inactivated by heating for 10 min at 95°C . The cDNA was diluted to a concentration equivalent to 2 ng/ μl equivalent RNA.

Quantitative-RT-PCR was performed using cDNA equivalent to 10 ng RNA in a total of 25 μl PCR mix. The total mix contained cDNA, 300 nM forward primer, 300 nM reverse primer, and 1 \times SYBRgreen PCR Master Mix. The 2 \times SYBRgreen PCR Master Mix [Applied Biosystems (ABI), Nieuwekerk a/d IJssel, The Netherlands] is optimized for SYBRgreen reactions and contains SYBRgreen I Dye, AmpliTaq Gold DNA Polymerase, deoxynucleotide triphosphates with dUTP, passive reference, and optimized buffer components. The Q-PCR was performed in a MicroAmp optical 96-well reaction plate (Applied Biosystems) with an ABI prism optical adhesive cover in the ABI PRISM 7900HT sequence detection system. The program used was 10 min at 95°C (100% ramp), 40 cycles of 15 sec at 95°C (100% ramp), and 1 min at 60°C (100% ramp), followed by a dissociation curve step of 15 sec at 95°C (100% ramp), 15 sec at 60°C (100% ramp), and 15 sec at 95°C (2% ramp).

The following forward (F) and reverse (R) primer pairs were used: DUSP1-354F, 5'-CAACGAGGCCATTGACTTCATA-3'; DUSP1-422R, 5'-GCCTGGCAGTGGACAAACA-3'; Wnt5A-189F, 5'-CATGAACCTGCACAACAACGA-3'; Wnt5A-296R, 5'-CAGCATGTCTTCAGGCTACATGA-3'; ADAMTS-1-75F, 5'-GCAGAGCACTATGACACAGCAAT-3'; ADAMTS-1-158R, 5'-ATCAGCCATCCCAAGAGTATCAC-3'; TPA-170F, 5'-GGGCACAGTGCCACTCAGT-3'; TPA-272R, 5'-TGGCACACGAAATCTGAGAAGT-3'; PAI-240F, 5'-GGGTGAAGACACAC-

ACAAAAGGT-3'; PAI-352R, 5'-CTTCCACTGGCCGTTGAA-GTA-3'; Sfrp4-409F, 5'-GGACCTCCCGGAGGATGTTA-3'; Sfrp4-477R, 5'-TCAAGAGGCCTTCCTGTACCA-3'.

Microarray Hybridization, Data Processing, and Statistical Analysis

GeneChips HG_U133A and HG_U133B (Affymetrix, High Wycombe, UK), together encompassing more than 45,000 human DNA fragments, were hybridized at the Organon Gene Chip Platform (Newhouse, UK). Details of chip content are available at the NetAffx analysis center (<http://www.affymetrix.com/analysis/index.affx>) (66). Biotin-labeled cRNA, which was generated from eight different PCOS ovary samples, 22 TSX ovary samples, and 11 different normal ovary samples was fragmented and used for hybridizations according to Affymetrix protocols. Hybridized chips were scanned and data automigrated into Rosetta Resolver (Rosetta Biosoftware, Kirkland WA). A Chip Quality Report was evaluated for abnormal glyceraldehyde-3-phosphate dehydrogenase 3'-5' ratios, average background, and glyceraldehyde-3-phosphate dehydrogenase absolute signals.

PCA was performed with a guide ("Analyze experiments using PCA") within Spotfire DecisionSite 7.2 (Spotfire, Göteborg, Sweden). A representative set of 500 fragments was selected by K-means clustering. The resulting table of 500 rows (genes) and 41 columns (ovary samples) was transposed and PCA was run to detect and reduce the number variables to three principal components which represent the majority of the variability in the dataset. A three-dimensional scatterplot was produced to visualize the differences in sample type (*i.e.* PCOS or TSX or normal) based on each sample's gene expression profile.

Rosetta Resolver allows normalization of sample data after selection of the appropriate set of samples (*e.g.* PCOS and normal ovary samples) for calculation of one-way ANOVA. A one-way ANOVA with build ratio was calculated to identify changes in expression levels between the two sample sets. Three criteria were used to define genes that had altered mRNA abundance in PCOS or TSX: 1) the absolute fold change had to be 1.80, or 2) the corresponding *P* value for the fold change had to be 0.01 or less, and 3) the number of present calls within a sample group must be sufficiently high. All Affymetrix Microarray Suite version 5.0 (MAS5)-processed expression signals contain a corresponding *P* value for the significance of expression. A *P* value of 0.05 or less was considered as "present" and higher levels as "absent." For up-regulated genes in PCOS samples, at least six of eight samples should have present calls and for down-regulated genes in PCOS at least eight of 11 normal samples should have present calls. The TSX sample group must contain at least 16 present calls for the TSX up-regulated genes. With the list of PCOS deregulated genes we searched gene by gene in the Ovarian Kaleidoscope database (<http://ovary.stanford.edu/>) (67) for additional information on ovarian biology that might be relevant in our studies. This database provides information regarding the biological function, expression pattern, and regulation of genes expressed in the ovary. When applicable, this supplementary information is appended.

Acknowledgments

We thank Dr. J. Strauss III and Dr. A. Hsueh for critically reading the manuscript and providing helpful suggestions.

Received February 20, 2004. Accepted August 5, 2004.

Address all correspondence and requests for reprints to: Erik Jansen, NV Organon, PO Box 20, 5340 BH Oss, The Netherlands. E-mail: erik.jansen@organon.com.

The authors have declared that no conflict of interest exists.

REFERENCES

1. The Rotterdam ESHRE/ASRM sponsored PCOS consensus workshop group 2004 Revised 2003 consensus on diagnostic criteria and long-term health risks related to polycystic ovary syndrome (PCOS). *Hum Reprod* 19: 41–47
2. The Rotterdam ESHRE/ASRM sponsored PCOS consensus workshop group 2004 Revised 2003 consensus on diagnostic criteria and long-term health risks related to polycystic ovary syndrome. *Fertil Steril* 81:19–25
3. Rowe PJ, Comhaire FH, Hargreave TB, Mellows HJ 1993 WHO manual for the standardized investigation and diagnosis of the infertile couple. Cambridge, UK: Cambridge University Press; 1–67
4. Knochenhauer ES, Key TJ, Kahsar-Miller M, Waggoner W, Boots LR, Azziz R 1998 Prevalence of the polycystic ovary syndrome in unselected black and white women of the southeastern United States: a prospective study. *J Clin Endocrinol Metab* 83:3078–3082
5. Solomon CG 1999 The epidemiology of polycystic ovary syndrome. Prevalence and associated disease risks. *Endocrinol Metab Clin North Am* 28:247–263
6. Adams J, Franks S, Polson DW, Mason HD, Abdulwahid N, Tucker M, Morris DV, Price J, Jacobs HS 1986 Multifollicular ovaries: clinical and endocrine features and response to pulsatile gonadotropin releasing hormone. *Lancet* 326:1375–1379
7. Pache TD, Hop WC, de Jong FH, Leerentveld RA, van Geldorp H, Van de Kamp TM, Gooren LJ, Fauser BC 1992 17 β -Oestradiol androstenedione and inhibin levels in fluid from individual follicles of normal and polycystic ovaries and in ovaries from androgen treated female to male transsexuals. *Clin Endocrinol (Oxf)* 36:565–571
8. Balen A, Laven JS, Tan SL, Dewailly D 2003 Ultrasound assessment of the polycystic ovary: international consensus definitions. *Hum Reprod Update* 9:505–514
9. Hughesdon PE 1982 Morphology and morphogenesis of the Stein-Leventhal ovary and of so-called "hyperthecosis." *Obstet Gynecol Surv* 37:59–77
10. Webber LJ, Stubbs S, Stark J, Trew GH, Margara R, Hardy K, Franks S 2003 Formation and early development of follicles in the polycystic ovary. *Lancet* 362: 1017–1021
11. Laven JS, Mulders AG, Visser JA, Themmen AP, de Jong FH, Fauser BC 2004 Anti-Müllerian hormone serum concentrations in normo-ovulatory and anovulatory women of reproductive age. *J Clin Endocrinol Metab* 89:318–323
12. Nelson VL, Legro RS, Strauss III JF, McAllister JM 1999 Augmented androgen production is a stable steroidogenic phenotype of propagated theca cells from polycystic ovaries. *Mol Endocrinol* 13:946–957
13. Wood JR, Nelson VL, Ho C, Jansen E, Wang CY, Urbanek M, McAllister JM, Mosselman S, Strauss III JF 2003 The molecular phenotype of polycystic ovary syndrome (PCOS) theca cells and new candidate PCOS genes defined by microarray analysis. *J Biol Chem* 278: 26380–26390
14. Legro RS, Spielman R, Urbanek M, Driscoll D, Strauss III JF, Dunaif A 1998 Phenotype and genotype in polycystic ovary syndrome. *Recent Prog Horm Res* 53:217–256
15. Crosignani PG, Nicolosi AE 2001 Polycystic ovarian disease: heritability and heterogeneity. *Hum Reprod Update* 7:3–7
16. Legro RS, Strauss III JF 2002 Molecular progress in infertility: polycystic ovary syndrome. *Fertil Steril* 78: 569–576

17. Hartley PS, Bayne RA, Robinson LL, Fulton N, Anderson RA 2002 Developmental changes in expression of myeloid cell leukemia-1 in human germ cells during oogenesis and early folliculogenesis. *J Clin Endocrinol Metab* 87:3417–3727
18. Teixeira Filho FL, Barakat EC, Lee TH, Suh CS, Matsui M, Chang RJ, Shimasaki S, Erickson GF 2002 Aberrant expression of growth differentiation factor-9 in oocytes of women with polycystic ovary syndrome. *J Clin Endocrinol Metab* 87:1337–1344
19. Hourvitz A, Kuwahara A, Hennebold JD, Tavares AB, Negishi H, Lee TH, Erickson GF, Adashi EY 2002 The regulated expression of the pregnancy-associated plasma protein-A in the rodent ovary: a proposed role in the development of dominant follicles and of corpora lutea. *Endocrinology* 143:1833–1844
20. Jakimiuk AJ, Weitsman SR, Navab A, Magoffin DA 2001 Luteinizing hormone receptor steroidogenesis acute regulatory protein and steroidogenic enzyme messenger ribonucleic acids are overexpressed in thecal and granulosa cells from polycystic ovaries. *J Clin Endocrinol Metab* 86:1318–1323
21. Wickenheisser JK, Quinn PG, Nelson VL, Legro RS, Strauss III JF, McAllister JM 2000 Differential activity of the cytochrome P450 17 α -hydroxylase and steroidogenic acute regulatory protein gene promoters in normal and polycystic ovary syndrome theca cells. *J Clin Endocrinol Metab* 85:2304–2411
22. Daneshmand S, Weitsman SR, Navab A, Jakimiuk AJ, Magoffin DA 2002 Overexpression of theca-cell messenger RNA in polycystic ovary syndrome does not correlate with polymorphisms in the cholesterol side-chain cleavage and 17 α -hydroxylase/C(17–20) lyase promoters. *Fertil Steril* 77:274–280
23. Dunaif A 1997 Insulin resistance and the polycystic ovary syndrome: mechanism and implications for pathogenesis. *Endocr Rev* 18:774–800
24. Waterworth DM, Bennett ST, Gharani N, McCarthy MI, Hague S, Batty S, Conway GS, White D, Todd JA, Franks S, Williamson R 1997 Linkage and association of insulin gene VNTR regulatory polymorphism with polycystic ovary syndrome. *Lancet* 349:986–990
25. Haddad L, Evans JC, Gharani N, Robertson C, Rush K, Wiltshire S, Frayling TM, Wilkin TJ, Demaine A, Millward A, Hattersley AT, Conway G, Cox NJ, Bell GI, Franks S, McCarthy MI 2002 Variation within the type 2 diabetes susceptibility gene calpain-10 and polycystic ovary syndrome. *J Clin Endocrinol Metab* 87:2606–2610
26. Bowtell DD 1999 Options available—from start to finish—for obtaining expression data by microarray. *Nat Genet* 21(Suppl 1):25–32
27. Golub TR, Slonim DK, Tamayo P, Huard C, Gaasenbeek M, Mesirov JP, Coller H, Loh ML, Downing JR, Caligiuri MA, Bloomfield CD, Landers ES 1999 Molecular classification of cancer: class discovery and class prediction by gene expression monitoring. *Science* 286:531–537
28. Lock C, Hermans G, Pedotti R, Brendolan A, Schadt E, Garren H, Langer-Gould A, Strober S, Cannella B, Allard J, Klonowski P, Austin A, Lad N, Kaminski N, Galli SJ, Oksenberg JR, Raine CS, Heller R, Steinman L 2002 Gene-microarray analysis of multiple sclerosis lesions yields new targets validated in autoimmune encephalomyelitis. *Nat Med* 8:500–508
29. Sreekumar R, Halvatsiotis P, Schimke JC, Nair KS 2002 Gene expression profile in skeletal muscle of type 2 diabetes and the effect of insulin treatment. *Diabetes* 51:1913–1920
30. Pache TD, Chadha S, Gooren LJ, Hop WC, Jaarsma KW, Dommerholt HB, Fauser BC 1991 Ovarian morphology in long-term androgen-treated female to male transsexuals. A human model for the study of polycystic ovarian syndrome? *Histopathology* 19:445–452
31. Jolliffe IT 1986 Principal component analysis. Springer series in statistics. New York: Springer-Verlag; 1–271
32. Park JI, Park HJ, Lee YI, Seo YM, Chun SY 2002 Regulation of NGFI-B expression during the ovulatory process. *Mol Cell Endocrinol* 202:25–29
33. Sterneck E, Tessarollo L, Johnson PF 1997 An essential role for C/EBP β in female reproduction. *Genes Dev* 11:2153–2162
34. Jirawatnotai S, Moons DS, Stocco CO, Franks R, Hales DB, Gibori G, Kiyokawa H 2003 The cyclin-dependent kinase inhibitors p27Kip1 and p21Cip1 cooperate to restrict proliferative life span in differentiating ovarian cells. *J Biol Chem* 278:17021–17027
35. Gonzalez-Robayna IJ, Alliston TN, Buse P, Firestone GL, Richards JS 1999 Functional and subcellular changes in the A-kinase-signaling pathway: relation to aromatase and Sgk expression during the transition of granulosa cells to luteal cells. *Mol Endocrinol* 13:1318–1337
36. Hsieh M, Mulders SM, Friis RR, Dharmarajan A, Richards JS 2003 Expression and localization of secreted frizzled-related protein-4 in the rodent ovary: evidence for selective up-regulation in luteinized granulosa cells. *Endocrinology* 144:4597–4606
37. Maiti S, Doskow J, Li S, Nhim RP, Lindsey JS, Wilkinson MF 1996 The *Pem* homeobox gene androgen-dependent and -independent promoters and tissue-specific alternative RNA splicing. *J Biol Chem* 271:17536–17546
38. Geserick C, Weiss B, Schleuning WD, Haendler B 2002 OTEX an androgen-regulated human member of the paired-like class of homeobox genes. *Biochem J* 366:367–375
39. Zorn AM 2001 Wnt signalling: antagonistic dickkopfs. *Curr Biol* 11:R592–R595
40. Moeller C, Swindell EC, Kispert A, Eichele G 2003 Carboxypeptidase Z (CPZ) modulates Wnt signaling and regulates the development of skeletal elements in the chicken. *Development* 130:5103–5111
41. Hsieh M, Johnson MA, Greenberg NM, Richards JS 2002 Regulated expression of Wnts and Frizzleds at specific stages of follicular development in the rodent ovary. *Endocrinology* 143:898–908
42. Ricken A, Lochhead P, Kontogiannea M, Farookhi R 2002 Wnt signaling in the ovary: identification and compartmentalized expression of wnt-2 wnt-2b and frizzled-4 mRNAs. *Endocrinology* 143:2741–2749
43. Ries A, Gohring W, Fox JW, Timpl R, Sasaki T 2001 Recombinant domains of mouse nidogen-1 and their binding to basement membrane proteins and monoclonal antibodies. *Eur J Biochem* 268:5119–5128
44. Bukulmez O, Arici A 2000 Leukocytes in ovarian function. *Hum Reprod Update* 6:1–15
45. Mori T 1990 Immuno-endocrinology of cyclic ovarian function. *Am J Reprod Immunol* 24:80–89
46. Lanzavecchia A 1990 Receptor-mediated antigen uptake and its effect on antigen presentation to class II-restricted T lymphocytes. *Annu Rev Immunol* 8:773–793
47. Khoury EL, Marshall LA 1990 Luteinization of human granulosa cells in vivo is associated with expression of MHC class II antigens. *Cell Tissue Res* 262:217–224
48. Fujiwara H, Ueda M, Imai K, Fukuoka M, Yasuda K, Takakura K, Suginami H, Kanzaki H, Inoko H, Mori T 1993 Human leukocyte antigen-DR is a differentiation antigen for human granulosa cells. *Biol Reprod* 49:705–715
49. Suzuki T, Sasano H, Takaya R, Fukaya T, Yajima A, Date F, Nagura H 1998 Leukocytes in normal-cycling human ovaries: immunohistochemical distribution and characterization. *Hum Reprod* 13:2186–2191
50. Guicciardi ME, Gores GJ 2003 AIP1: a new player in TNF signaling. *J Clin Invest* 111:1813–1815
51. Grell M, Zimmermann G, Gottfried E, Chen CM, Grunwald U, Huang DC, Wu Lee YH, Durkop H, Engelmann H, Scheurich P, Wajant H, Strasser A 1999 Induction of cell death by tumour necrosis factor (TNF) receptor 2 CD40

- and CD30: a role for TNF-R1 activation by endogenous membrane-anchored TNF. *EMBO J* 18:3034–3043
52. Laven JS, Imani B, Eijkemans MJ, de Jong FH, Fauser BC 2001 Absent biologically relevant associations between serum inhibin B concentrations and characteristics of polycystic ovary syndrome in normogonadotrophic anovulatory infertility. *Hum Reprod* 16:1359–1364
 53. Gottlicher M, Minucci S, Zhu P, Kramer OH, Schimpf A, Giavara S, Sleeman JP, Lo Coco F, Nervi C, Pelicci PG, Heinzel T 2001 Valproic acid defines a novel class of HDAC inhibitors inducing differentiation of transformed cells. *EMBO J* 20:6969–6979
 54. Chang T, Szabo E 2002 Enhanced growth inhibition by combination differentiation therapy with ligands of peroxisome proliferator-activated receptor- γ and inhibitors of histone deacetylase in adenocarcinoma of the lung. *Clin Cancer Res* 8:1206–1212
 55. Lampen A, Siehler S, Ellerbeck U, Gottlicher M, Nau H 1999 New molecular bioassays for the estimation of the teratogenic potency of valproic acid derivatives in vitro: activation of the peroxisomal proliferator-activated receptor (PPAR δ). *Toxicol Appl Pharmacol* 160:238–249
 56. Isojarvi JI, Tauboll E, Pakarinen AJ, van Parys J, Rattya J, Harbo HF, Dale PO, Fauser BC, Gjerstad L, Koivunen R, Knip M, Tapanainen JS 2001 Altered ovarian function and cardiovascular risk factors in valproate-treated women. *Am J Med* 111:290–296
 57. Betts T, Yarrow H, Dutton N, Greenhill L, Rolfe T 2003 A study of anticonvulsant medication on ovarian function in a group of women with epilepsy who have only ever taken one anticonvulsant compared with a group of women without epilepsy. *Seizure* 12:323–329
 58. Nelson-deGrave V, Wickenheisser JK, Cockrell JE, Wood JR, Legro RS, Strauss III JF, McAllister JM 2004 Valproate potentiates androgen biosynthesis in human ovarian theca cells. *Endocrinology* 145:799–808
 59. Hara M, Alcoser SY, Qaadir A, Beiswenger KK, Cox NJ, Ehrmann DA 2002 Insulin resistance is attenuated in women with polycystic ovary syndrome with the Pro¹²Ala polymorphism in the PPAR γ gene. *J Clin Endocrinol Metab* 87:772–775
 60. Korhonen S, Heinonen S, Hiltunen M, Helisalmi S, Hippelainen M, Koivunen R, Tapanainen JS, Laakso M 2003 Polymorphism in the peroxisome proliferator-activated receptor- γ gene in women with polycystic ovary syndrome. *Hum Reprod* 18:540–543
 61. Orio Jr F, Matarese G, Di Biase S, Palomba S, Labella D, Sanna V Savastano S, Zullo F, Colao A, Lombardi G 2003 Exon 6 and 2 peroxisome proliferator-activated receptor- γ polymorphisms in polycystic ovary syndrome. *J Clin Endocrinol Metab* 88:5887–5892
 62. Urbanek M, Legro RS, Driscoll DA, Azziz R, Ehrmann DA, Norman RJ, Strauss III JF, Spielman RS, Dunaif A 1999 Thirty-seven candidate genes for polycystic ovary syndrome: strongest evidence for linkage is with follistatin. *Proc Natl Acad Sci USA* 96:8573–8578
 63. Urbanek M, Legro RS, Driscoll D, Strauss III JF, Dunaif A, Spielman RS 2000 Searching for the polycystic ovary syndrome genes. *J Pediatr Endocrinol Metab* 13(Suppl 5):1311–1313
 64. Blanchard DK, Hartmann LC 2000 Prophylactic surgery for women at high risk for breast cancer. *Clin Breast Cancer* 1:127–134
 65. van Santbrink EJ, Hop WC, Fauser BC 1997 Classification of normogonadotropic infertility: polycystic ovaries diagnosed by ultrasound versus endocrine characteristics of polycystic ovary syndrome. *Fertil Steril* 67:452–458
 66. Liu G, Loraine AE, Shigeta R, Cline M, Cheng J, Valmееkam V, Sun S, Kulp D, Siani-Rose MA 2003 NetAffx: Affymetrix probesets and annotations. *Nucleic Acids Res* 31:82–86
 67. Ben-Shlomo I, Vitt UA, Hsueh AJ 2002 Perspective: the ovarian kaleidoscope database-II. Functional genomic analysis of an organ-specific database. *Endocrinology* 143:2041–2044

